Stem Cell Reports
Article

ISSCR

OPEN ACCESS

Reprogramming of Fibroblasts to Oligodendrocyte Progenitor-like Cells Using CRISPR/Cas9-Based Synthetic Transcription Factors

Mantas Matjusaitis,[1] Laura J. Wagstaff,[1] Andrea Martella,[1] Bart Baranowski,[1] Carla Blin,[1] Sabine Gogolok,[1] Anna Williams,[1] and Steven M. Pollard[1,*]

[1]MRC Centre for Regenerative Medicine and Edinburgh Cancer Research UK Centre, University of Edinburgh, 5 Little France Drive, Edinburgh EH16 4UU, UK

*Correspondence: steven.pollard@ed.ac.uk

https://doi.org/10.1016/j.stemcr.2019.10.010

SUMMARY

Cell lineage reprogramming via transgene overexpression of key master regulatory transcription factors has been well documented. However, the poor efficiency and lack of fidelity of this approach is problematic. Synthetic transcription factors (sTFs)—built from the repurposed CRISPR/Cas9 system—can activate endogenous target genes to direct differentiation or trigger lineage reprogramming. Here we explored whether sTFs could be used to steer mouse neural stem cells and mouse embryonic fibroblasts toward the oligodendrocyte lineage. We developed a non-viral modular expression system to enable stable multiplex delivery of pools of sTFs capable of transcriptional activation of three key oligodendrocyte lineage master regulatory genes (*Sox10*, *Olig2*, and *Nkx6-2*). Delivery of these sTFs could enhance neural stem cell differentiation and initiated mouse embryonic fibroblast direct reprograming toward oligodendrocyte progenitor-like cells. Our findings demonstrate the value of sTFs as tools for activating endogenous genes and directing mammalian cell-type identity.

INTRODUCTION

New opportunities to directly manipulate endogenous gene expression in mammalian cells have emerged from the fields of genome editing and synthetic biology, including: synthetic transcription factors (sTFs) or chromatin editors, as well as improved DNA synthesis, assembly, and delivery methods. sTFs are engineered chimeric proteins containing a DNA-binding domain fused to transcriptional or chromatin regulatory effector domains. sTFs were pioneered using zinc-finger transcription factors (reviewed in Keung et al. [2015]). CRISPR/Cas9 has emerged as a preferred platform for manufacture of sTFs (Gilbert et al., 2013). Catalytically dead Cas9 (dCas9)—a nuclease-deficient variant of Cas9 endonuclease—retains site-specific binding but lacks DNA cutting activity. dCas9, therefore, still binds via the complementarity of a short guide RNA (sgRNA) to predetermined target DNA sequence yet does not cleave the DNA. When tethered to transcriptional activation domains, such as VP160, the resulting programmable dCas9-based sTF is able to activate target gene transcription (Perez-Pinera et al., 2013; Cheng et al., 2013). sTFs based on the dCas9 architecture can therefore be used to drive cell lineage programming or differentiation via activation of endogenous master regulatory transcription factors.

Several recent examples of sTF-directed control of mammalian cell differentiation have been described for pluripotent cell differentiation (embryonic stem cells [ESCs] or induced pluripotent stem cells [iPSCs]) including neurons, trophoblast stem cells, or pancreatic lineages (Balboa et al., 2015; Chavez et al., 2015). sTFs have also been used to drive lineage conversions by targeting a single master regulator, e.g., activation of *MyoD* to drive fibroblast reprogramming to skeletal myocytes (Chakraborty et al., 2014); and, recently, remodeling of the *Sox2* locus to trigger reprogramming of fibroblasts to iPSCs (Liu et al., 2018). Multiplex gene activation is more challenging. However, Black et al. (2016) demonstrated successful direct lineage conversion of fibroblasts to neurons by simultaneous sTF-based activation of *Ascl1*, *Pou3f2*, and *Myt1l* using cocktails of lentiviral vectors.

Despite these successes, important barriers remain. More efficient strategies are needed to build plasmids containing multiple sTFs. This remains challenging due to repetitive sequences inherent to sgRNA structure. It also remains challenging to stably deliver cocktails of multiple sTFs. At present, only lentiviral systems, with their inherent limitations in cargo size, or Gateway cloning-based systems—which have a low number of unique cloning sites—have been used to construct sTFs targeting multiple genes for cell lineage programming. Each of these approaches has restrictions for multiplexing. It is also uncertain whether multiplex activation and direct lineage reprogramming with sTFs will be robust and reliable for lineage conversions other than fibroblasts to neurons (Black et al., 2016).

One clinically important cell type is the oligodendrocyte (OL), which is disrupted in demyelinating diseases (Franklin and Ffrench-Constant, 2017). OLs and their oligodendrocyte progenitor cell (OPC) are potentially attractive targets for cell-based therapies and disease modeling, as their functional properties are less diverse and region/subtype specific than neurons. Differentiation of human iPSCs to OLs has been achieved and has provided

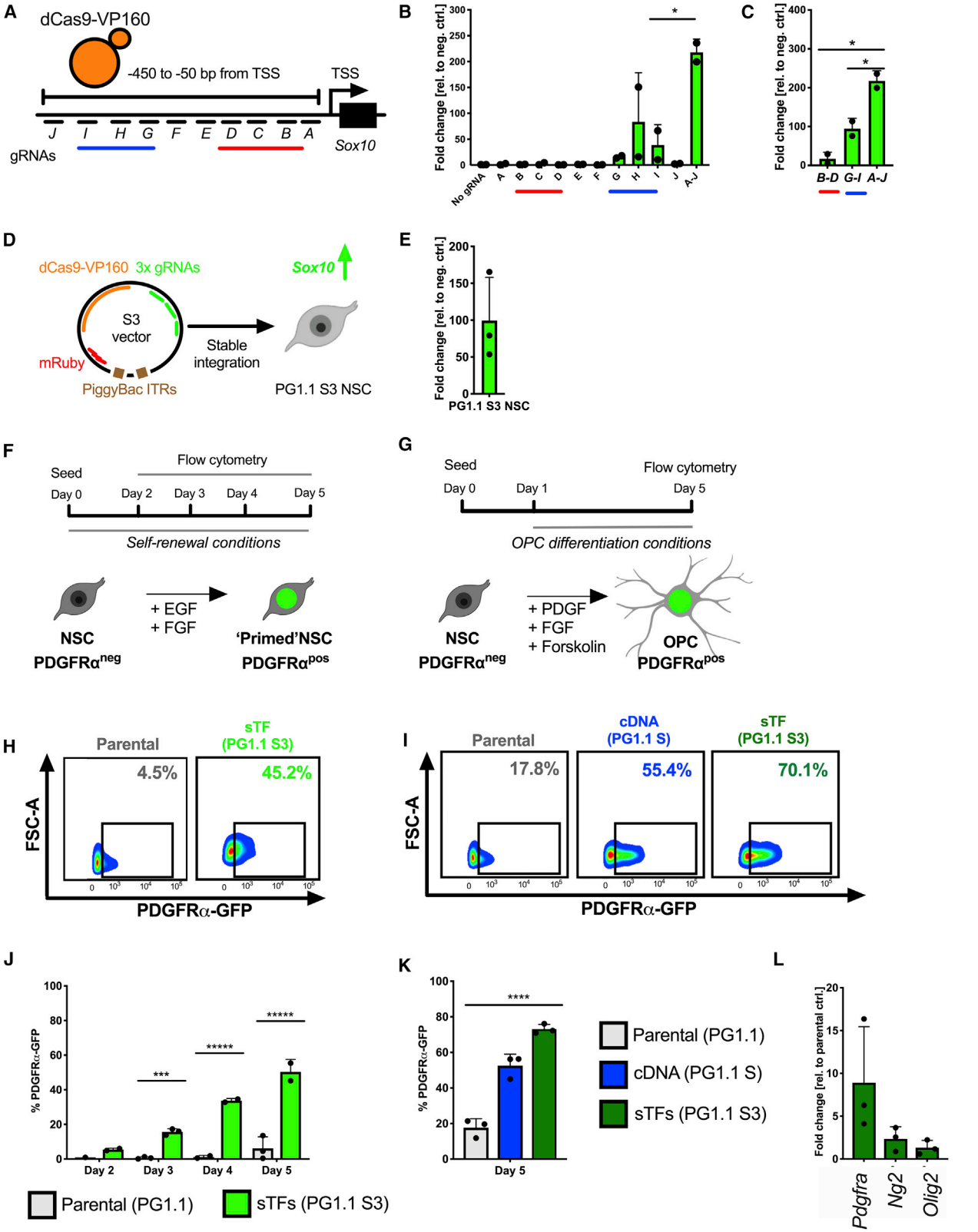

(legend on next page)

proof-of-principle of the functional properties of these cells after transplantation (Goldman, 2016). Also, direct lineage conversion of fibroblasts to generate OPCs has been demonstrated by viral overexpression of OLIG2, SOX10, and NKX6-2 (Najm et al., 2013), providing a more direct route to OL production *ex vivo*.

Here we tested whether sTFs can be used to facilitate cell fate programming toward OLs in neural stem cells (NSCs) and mouse embryonic fibroblasts (MEFs). We developed an improved modular cloning strategy to facilitate construction of single plasmids that can carry up to eight gRNAs plus dCas9-VP160 and delivered these efficiently and stably into primary NSCs or fibroblasts using a transposase-based approach. We show that sTF-based activation of *Sox10* in NSCs will trigger specification to OPCs and OLs. Furthermore, we also demonstrate that fibroblast reprogramming to MBP-expressing OL-like cells can be achieved by sTF-based activation of three major OL lineage regulators: *Sox10*, *Olig2*, and *Nkx6-2*.

RESULTS

Activation of Endogenous *Sox10* in Mouse NSCs Using dCas9/sgRNAs

Sox10 is a known regulator of OL specification and differentiation in development, differentiating PSCs, and cultured NSCs (García-León et al., 2018; Stolt et al., 2006; Wang et al., 2013). We first explored whether dCas9-VP160 can activate *Sox10* transcription in mouse NSCs, and whether this influenced their subsequent differentiation into OLs.

We screened 10 individual gRNAs located −450 to −50 bp upstream of *Sox10* transcription start site (TSS) (Figure 1A). Targeting this region was previously shown to generate most functional gRNAs (Gilbert et al., 2014). Individual or pools of gRNAs were co-transfected with dCas9-VP160 in NSCs (Figure 1B). Three gRNAs were identified that could increase levels of *Sox10* mRNA by ∼10-fold when delivered individually (*G*, *H*, and *I*). However, we found that co-transfection of a pool of all 10 gRNAs (*A*–*J*) gave >217-fold increase in mRNA (Figure 1B). A synergistic effect was also seen when co-transfecting a pool of the three individually most potent gRNAs together with dCas9-VP160 (*G*–*I*) (Figure 1C). This is consistent with findings from previous reports that showed co-delivery of multiple gRNAs can significantly increase transcription of the target gene, likely via some synergistic effect (Black et al., 2016; Perez-Pinera et al., 2013). Concomitant delivery of multiple sTFs may, therefore, provide the most robust strategy to activate target gene expression. Furthermore, transcription activation and overexpression of the target gene with dCas9-VP160 is a transient phenomenon as almost no *Sox10* mRNA could be detected 12 days after transfection (Figure S2G).

Targeting of multiple "master regulators" would likely be required for sTFs to be effective in direct reprogramming. Next, we designed a plasmid-based expression system that could enable simultaneous delivery of gRNAs against

Figure 1. Activation of Endogenous *Sox10* Transcription in Neural Stem Cells and Specification to Oligodendrocyte Precursor Cells

(A) Schematic representation of the sgRNA target positions designed for transcriptional activation of *Sox10*. Ten gRNAs spanning the proximal *Sox10* promoter (−400 to −50 bp from TSS) were tested (termed *A* through to *J*).

(B and C) qRT-PCR results for *Sox10* mRNA in NSCs (PDGFRα-GFP reporter cells; termed PG1.1) 3 days after the co-transfection with gRNAs and dCas9-VP160. (B) Single co-transfected gRNAs (*A*, *B*, *C*, etc.) compared with a pool of 10 co-transfected gRNAs (n = 2; ordinary one-way ANOVA p = 0.0004). (C) Comparison of pools of three most active and three inactive gRNAs (n = 2; ordinary one-way ANOVA p = 0.007). Negative control is cells transfected with dCas9-VP160 alone (No gRNAs).

(D) Schematic of "S3" plasmid containing 3 × gRNAs targeting *Sox10*, CAG-driven mRuby for selection and dCas9-VP160 with PiggyBac arms for stable integration into the genome of PG1.1 cells (PG1.1-S3).

(E) qRT-PCR for *Sox10* mRNA in PG1.1-S3 cells in self-renewal conditions (EGF plus FGF-2) 3 weeks after integration (n = 3; unpaired t test p = 0.04).

(F and G) Graphical representation of experimental design. Parental and sTF-containing PG1.1 NSCs were seeded at medium density (1.3×10^4 cell/cm^2) on day 0 to minimize spontaneous differentiation arising from high confluence. (F) Cells were left in self-renewal conditions (EGF and FGF) and checked for PDGFRα-GFP using flow cytometry every day until day 5. (G) Cells were induced to differentiate by removal of EGF and addition of PDGF-AA and Forskolin. Four days after differentiation induction, cells were scored for PDGFRα-GFP using flow cytometry.

(H and I) Typical example of flow cytometry at day 5 for PDGFRα-GFP in PG1.1 ("Parental"), PG1.1 S ("cDNA"), and PG1.1 S3 ("sTF") NSCs grown under (H) self-renewal conditions or (I) differentiation conditions.

(J and K) Quantification of flow cytometry data, either in (J) self-renewal conditions (n = 3; ordinary one-way ANOVA p < 0.0009) or (K) differentiation conditions (n = 3; unpaired t test p < 0.0001).

(L) qRT-PCR data for *Pdgfrα*, *Ng2*, and *Olig2* mRNA in PG1.1 S3 NSC ("sTF Sox10 × 3 gRNAs") 4 days after differentiation, normalized to differentiated parental PG1.1 cells (n = 3).

Statistical analysis—dots represent biological replicates, bars indicate means; error bar represent SD; unpaired t tests were performed. Statistical significance is marked by asterisks (*). See also Figures S1–S3.

many targets. An "all-in-one plasmid" (A1P) destination vector was built containing: (1) a CAG promoter-driven dCas9-VP160; (2) PiggyBac transposase recombination sites (for stable genomic integration); (3) a CAG promoter-driven mRuby-P2A-PuroR (for selection); and (4) an RFP cassette that is flanked by unique BsmBI sites for Golden Gate cloning of gRNAs (Figures 1D and S1A). Using an adapted version of our recently described extensible mammalian modular assembly system (Martella et al., 2017), we designed a simple workflow that allows assembly of multiple U6-sgRNA subunits into the A1P vector from the single sgRNA expression plasmids (Figure S1B). To test if recombination during plasmid preparation in bacteria compromises plasmid integrity, we have sub-cloned, picked, and sequenced multiple colonies. We have found no evidence of recombination in any of the clones (Figure S2F).

For functional validation of this design, we constructed plasmid A1P-S3, comprising three U6-gRNAs arrays, each with a distinct sgRNA against *Sox10*. This was stably integrated into NSCs by co-transfection with the pBase transposase (Figure 1D). Two weeks after transfection, cells with successfully integrated plasmids (±1%) were selected by sorting for mRuby. As expected, the resulting sTF-expressing NSCs robustly triggered increased expression of *Sox10* (Figure 1E). This A1P system can therefore be used to deliver sTFs to precise sites in the genome for target gene activation.

Sox10 Activation by sTFs Triggers Specification of NSCs to OPCs and OLs

Activation of *Sox10* in NSCs might bias differentiation to OLs. Platelet-derived growth factor receptor alpha (PDGFRα) is one of the earliest markers of OPCs. Therefore, we generated a reporter NSC line to monitor OPC lineage specification. An existing PDGFRα-H2B-GFP reporter transgenic mouse was used (Hamilton et al., 2003), and NSC cultures were established from embryonic 14.5 (E14.5) fetal forebrain (Figures S3A and S3B). We derived a clonal NSC line from this population, termed PG1.1, which is karyotypically normal and displays typical NSC morphology and markers (NESTIN, OLIG2, SOX2, and SOX9) (Figure S3C) (Conti et al., 2005). On differentiation, this reporter line accumulated nuclear GFP when assessed by microscopy and flow cytometry during differentiation (Figures S3D and S3E). Indeed, we find ~10%–20% of cells express GFP$^+$ cells at day 4 of differentiation and these expressed OPC markers (Figure S3F).

To determine if *Sox10* activation using sTFs can override self-renewal signals and trigger spontaneous OPC specification we compared sTF-induced *Sox10* cells with parental controls grown in epidermal growth factor (EGF)/fibroblast growth factor-2 (FGF-2)-containing culture medium (non-permissive for OPC specification). Between experiments, cells were passaged frequently (every 2 days) and at low confluence (<50%) to minimize spontaneous differentiation. During experiments, cells were seeded at mid-range confluence (1.3×10^4 cell/cm^2) and the frequency of PDGFRα-GFP$^+$ cells was scored by flow cytometry every 24 h for 5 days (Figure 1F). As expected, PG1.1 parental cells generated very few PDGFRα-GFP$^+$ OPCs under these conditions (~6% GFP cells by day 5; triggered by high cell confluence at this point). By contrast, cells harboring the sTFs for *Sox10* (PG1.1 S3) induced ~45% of GFP$^+$ cells by day 5 (Figures 1H and 1J).

NSCs typically differentiate into varying proportions of astrocytes, neurons, and OLs (Conti et al., 2005), but OL differentiation can be promoted by removal of EGF and addition of Forskolin, FGF, and PDGF-AA to the culture medium (Figure 1G) (Glaser et al., 2007). To compare sTFs with more traditional cDNA overexpression approaches, we have also created a stable PG1.1 cell line that constitutively overexpresses *SOX10* and named it PG1.1-S (Figure S3G). On differentiation in these more permissive conditions we found that ~70% of PG1.1 S3 cells (sTF-activated *Sox10* expression) and 52% of PG.1-S (cDNA overexpression of *SOX10*) became PDGFRα-GFP$^+$ after 4 days of differentiation (Figures 1I and 1K), whereas ~15% of parental PG1.1 NSCs were PDGFRα-GFP$^+$. Cells containing sTFs also had higher levels of *Ng2* and *Pdgfra* mRNA—known markers of OPCs (Figure 1L). We conclude that sTF-induced expression of endogenous *Sox10* primes NSCs for OPC specification in a similar way as *Sox10* cDNA overexpression (Pozniak et al., 2010).

To confirm these results in an independent NSC line and determine if sTF-induced *Sox10* could further enhance differentiation to OLs we used wild-type early passage NSC cultures (adult subventricular zone-derived Black6 strain NSCs; BL6-NS). During their differentiation to OLs, OPCs transit into post-mitotic cells that are marked by the surface marker O4 and are committed to OL differentiation (Zhang, 2001). *Sox10* transcriptional activation is less efficient in BL6 NSCs compared with PG1.1 NSCs (data not shown); therefore, a plasmid containing eight gRNAs (all-in-one [Ai1]-S8) was used instead. To create a stable cell line, BL6 cells were transfected with A1P-S8 plasmid and pBase transposase (Figure 2A). Two weeks after transfection, cells were sorted for mRuby to select cells with integrated plasmid (1.4%; Figure S2E). We found >926-fold increase in *Sox10* mRNA levels in BL6 S8 cells compared with parental non-transfected BL6 NS control cells (Figure 2B). Protein levels of SOX10 were also confirmed using western blot (Figure 2C). After over 20 passages, we have genotyped our cell line to validate that it has not lost expression cassettes due to recombination (Figure S4C). To test the effects of sTF on differentiation, we used an

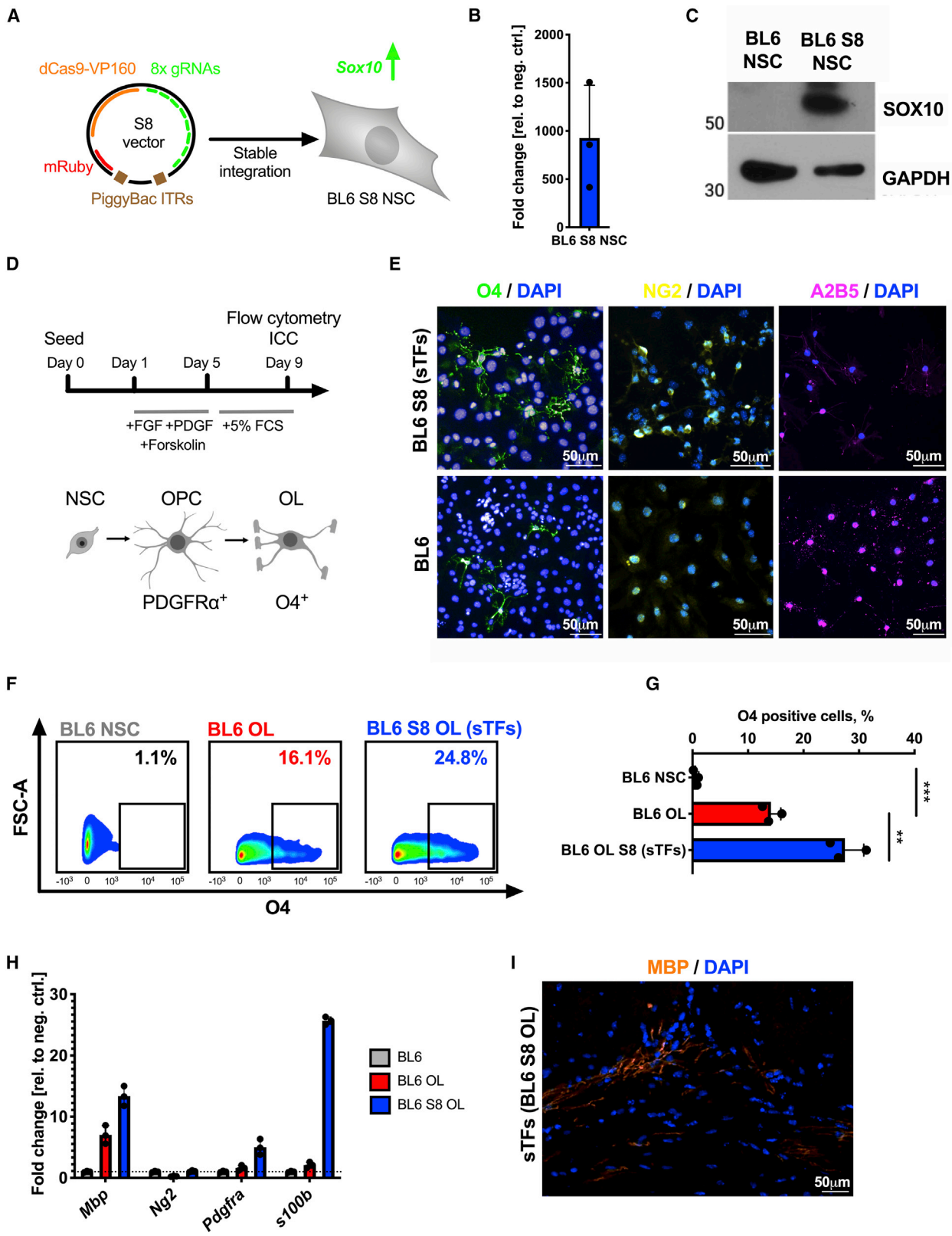

(legend on next page)

8-day two-step differentiation protocol (Figure 2D). Cells acquired a typical OL morphology and were immunopositive for O4, A2B5, and NG2 (Figure 2E). A ~2-fold increase in a number of $O4^+$ cells was observed in cells containing sTFs (on average, 14.1% for parental cells versus 27.4% for sTF-induced cells) (Figures 2F and 2G). Furthermore, these cells had higher mRNA levels of various OL-related genes such as *Mbp*, *Ng2*, *Pdgfrα*, and *s*100b (Figure 2H). There was no obvious difference between cell lines for GFAP and TUJ1 staining after differentiation (Figure S4B). Finally, BL6 S8 cells formed MBP^+ myelin sheaths after injection into the corpus callosum of shiverer MBPshi/shi mice (Figure 2I). Thus, activation of *Sox10* transcription in NSCs using sTFs can increase the frequency of OL lineage specification and differentiation commitment.

Simultaneous Transcriptional Activation of Endogenous *Sox10*, *Olig2*, and *Nkx6-2* in MEFs Using a Single Plasmid

We next explored whether sTFs could trigger reprogramming of fibroblasts to OPCs. Previous studies have shown that this is possible by viral cDNA overexpression of three transcriptional regulators *Sox10*, *Olig2*, and *Nkx6-2* or *Zfp536* (Najm et al., 2013; Yang et al., 2013). Activation of *Sox10* alone is therefore not sufficient for efficient reprogramming of fibroblasts to OPCs. We wished to extend our sTF approach to enable activation of multiple genes using multiple gRNAs simultaneously in the same cell.

We first tested each gene individually to identify sTFs that can activate target genes in MEFs. We designed ten different gRNAs for each of the three promoters (Figure 3A) and tested them individually by co-transfecting with dCas9-VP160 (Figures 3B–3D). For *Sox10* the same three gRNAs (*G*—*I*) that were functional in NSCs were also effective in MEFs (Figure 3B). Ten gRNAs for *Olig2* and *Nkx6-2* were tested in MEFs (Figures 3C and 3D), as well as NSCs (Figures S2A and S2B). For all three genes the most potent gRNAs were located <300 bp upstream of TSS. Surprisingly, the sTFs that activated *Nkx6-2* in MEFs did not work in NSCs (Figure S2B). This was not explained by the strength of the activation domain, as no significant transcription activation was observed even when VP160 was exchanged with stronger effectors, such as VPR (Chavez et al., 2015) and p300 (Hilton et al., 2015) (Figure S2C). This suggests significant cell-type-dependent requirements for testing and validating the sTFs.

Once again, we found that pools of gRNAs were more effective than any single gRNA (Figures 3B–3D). Multiplex delivery of combinations of two or three gRNAs gave the highest and most consistent activation for *Olig2* and *Nkx6-2*, reaching similar levels to pools of all ten gRNAs (Figure 3E). Thus, delivery of two or three gRNAs provides a reliable approach to activating target genes of interest in MEFs (Figure 3F). These validated gRNAs were built into a single expression plasmid enabling simultaneous multiplex activation of the three target genes (Figure 3G). We constructed three different A1P vectors with increasing numbers of gRNAs. The A1P-SON vector contained only three gRNAs in total, one for each gene (*Sox10*, *Olig2*, and *Nkx6-2*) (Figure 3G, blue bars); the A1P 2SON vector had two gRNAs for *Sox10* and *Olig2* and a single for *Nkx6-2* (Figure 3G, violet bars); and, finally, the A1P 3SON vector had three gRNAs for *Sox10* and *Olig2* and two gRNAs for *Nkx6-2* (Figure 3G, yellow bars). Two *Nkx6-2* gRNAs were chosen as this was sufficient to reach >100-fold activation in MEFs (Figure 3E), thereby providing similar levels of activation to *Olig2* and *Sox10*.

Head-to-head comparisons of these three different plasmids confirmed that increasing the number of functional gRNAs correlated with higher levels of target gene transcriptional activation (as seen with *Sox10* gene in particular). Strongest activation was observed using multiple gRNAs: *Sox10* from 2.7-fold change (1 sgRNA) to 141-fold change (3 gRNAs); *Olig2* from 24-fold (1 sgRNA) change to 69-fold change (3 gRNAs); *Nkx6-2* from 193-fold (1 sgRNA) change to 197-fold change (2 gRNAs) (Figure 3G).

Figure 2. Effect of sTF-Based *Sox10* Transcription Activation on Neural Stem Cell Differentiation to Oligodendrocytes

(A) Plasmid S8 containing eight gRNAs targeting *Sox10* and dCas9-VP160 was stably integrated into a wild-type BL6 NSC line (BL6 S8 NSC).

(B) qRT-PCR data showing levels of *Sox10* mRNA in BL6 S8 stable cell line 2 weeks after transfection (n = 3; unpaired t test p = 0.04).

(C) Western blot demonstrating SOX10 protein levels in BL6 and BL6 S8 cell lines.

(D) Schematic summarizing the experimental strategy.

(E) Immunofluorescent images after O4, A2B5, and NG2 staining on differentiated BL6 S8 NSC at day 9.

(F) Example of flow cytometry data for O4 surface protein (oligodendrocyte marker) of BL6 and BL6 S8 NSC at day 9.

(G) Quantification of flow cytometry of three different differentiation experiments as described in (C) (n = 3; ordinary one-way ANOVA p < 0.0001).

(H) qRT-PCR data of BL6 cells in self-renewal ("BL6"), differentiated BL6 cells ("BL6 OL"), and differentiated BL6 S8 cells ("BL6 S8 OL") after 8 days of differentiation (n = 3; unpaired t test).

(I) Immunofluorescent images of MBP staining of *Shiverer* MBPshi/shi mice brain section 21 days after BL6 S8 cells were transplanted into P2 mice.

Statistical analysis—dots represent biological replicates, bars indicate means; error bar represent SD; unpaired t tests were performed. Statistical significance is marked by asterisks (*). See also Figures S2 and S4.

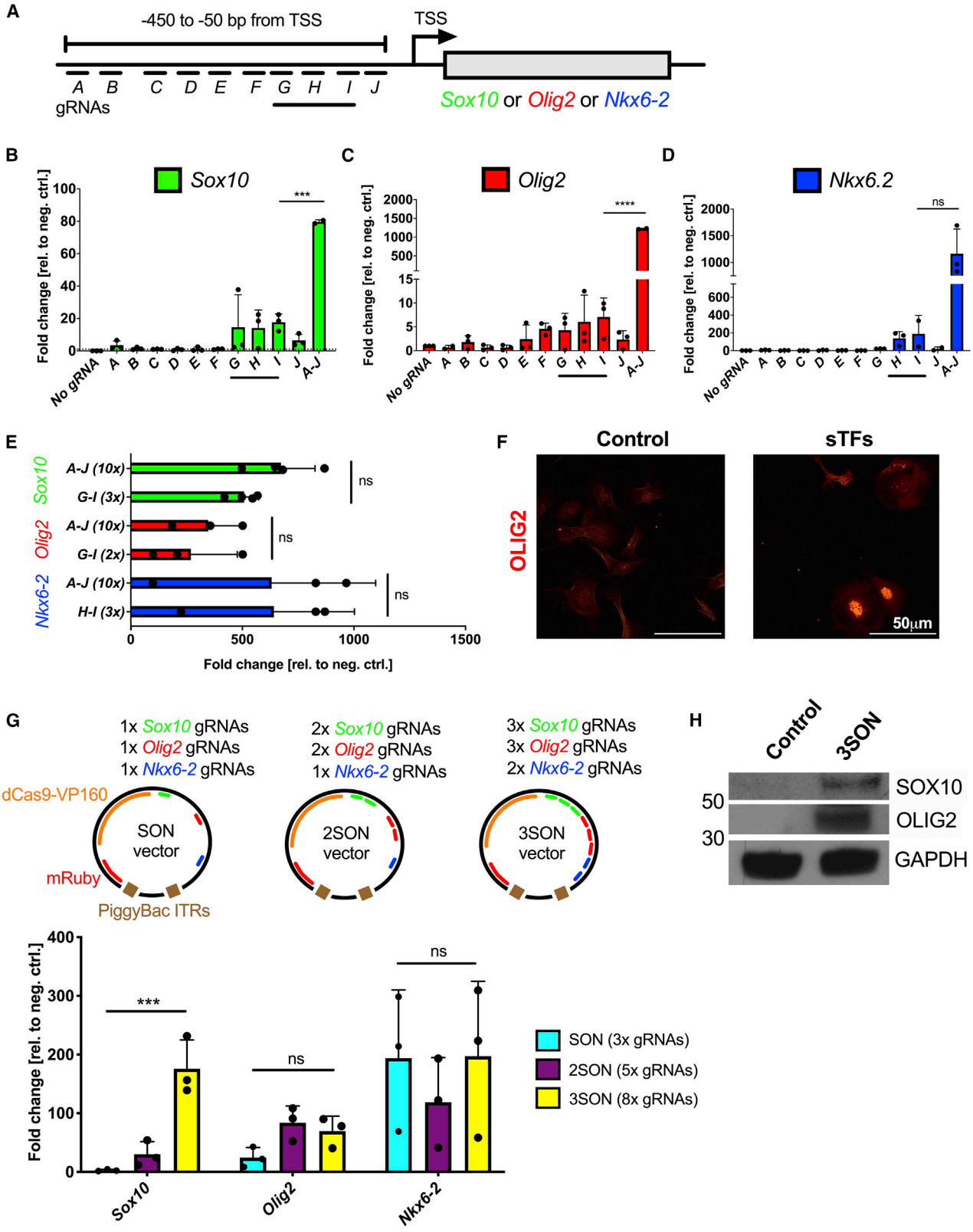

(legend on next page)

The "A1P-3SON" plasmid therefore enables strong transcription activation of all three factors to a similar extent at mRNA (Figure 3G) and protein (Figure 3H) level, but does not activate neighboring genes (*Polr2f*, *Olig1*, and *Cfap46*) (Figure S2D).

Simultaneous Activation of *Sox10*, *Olig2*, and *Nkx6-2* with sTFs Initiates Direct Reprogramming of Mouse Fibroblasts to MBP-Expressing OL-like Cells

With the validated plasmids for multiplex activation of *Sox10*, *Olig2*, and *Nkx6-2* in hand, we next tested whether delivery of the sTFs could drive MEF transdifferentiation (TD) to OPCs. For this, we generated fresh primary MEFs from distal limbs of E12.5 mouse embryos to avoid the risk of contamination of spinal cord-derived NSCs or OPCs. The resulting cultures displayed the typical MEF morphology and by qRT-PCR did not express NSC and OPC marker genes (Figures S5A and S5B). We stably co-transfected MEFs and switched to TD medium 3 days later (see Experimental Procedures for details of medium composition). Immunocytochemistry, flow cytometry, and qRT-PCR were used to score cells after 24 days (Figure 4A).

MEFs were transfected with three plasmids: A1P-3SON (containing eight gRNAs for *Sox10*, *Olig2*, and *Nkx6-2*), A1P-S8 (containing eight gRNAs for *Sox10*), and CAG-driven pBase transposase. From day 14 onward (peaking at day 24) we noted cells undergoing morphological changes resembling OPCs in the sTF-expressing cells, but not in non-transfected MEF controls (Figure 4B). Importantly, we observed the emergence of $O4^+$ cells in cells transfected with sTFs (plasmids A1P-3SON and A1P-S8; A1P-3SON alone was less efficient), while control MEFs were negative for both markers (Figure 4C). Quantification confirmed sTF-expressing cells had on average 8.9% $O4^+$ cells; controls (MEFs in MEF medium and MEFs in TD medium) were <1% $O4^+$ cells (Figure 4D).

Although we cannot quantify the efficiency of reprogramming directly because of cell death and cell replication during TD, in relative terms this efficiency is comparable with previous reports using viral cDNA overexpression: 9.2% (Najm et al., 2013) and 15.6% (Yang et al., 2013) of $O4^+$ cells. If we would be able to increase integration and/or transfection efficiency (currently less than 1% and 30%, respectively; Figure S5C) to that achieved with viral delivery in previous studies, reprogramming efficiency using sTFs might surpass that of cDNA overexpression.

We harvested $O4^+$ cells after 24 days using fluorescence-activated cell sorting (FACS) and extracted mRNA for qRT-PCR. This confirmed upregulation of many OL lineage markers, such as *Mbp*, *Cspg4* (*Ng2*), and *Nkx2-2*, and also the expected *Sox10*, *Olig2*, and *Nkx6-2* (Figure 4E). To check if the reprogramming process gave raise to other astrocytes or neuronal cells, we performed immunostaining for TUJ1, GFAP, and NESTIN at day 24 (Figure S4A). Only a few isolated $TUJ1^+$ cells were observed in both conditions (likely a remnant of peripheral neurons during MEF harvesting). Although we have identified some MBP^+ cells, these were infrequent *in vitro*, and therefore *in vivo* experiments were performed next.

To test if the induced oligodendrocyte progenitor-like cells (iOPCs) were able to integrate into mouse brain and contribute to myelin formation we performed the following experiments (Figure 5A). Firstly, we transdifferentiated cells after transfecting them with either sTFs (Ai1-3SON and Ai1-S8) and GFP-expressing plasmids ("With sTF") or just GFP-expressing plasmids ("No sTF"). Twenty-one days after TD induction, we transplanted cells

Figure 3. *Sox10*, *Olig2*, and *Nkx6-2* Activation Using sTFs in Mouse Embryonic Fibroblasts

(A) Schematic representation of the sgRNA target positions designed for transcriptional activation of *Sox10*, *Olig2*, and *Nkx6-2*. Ten gRNAs spanning the proximal promoters of *Sox10*, *Olig2*, and *Nkx6-2* (−400 to −50 bp from TSS) were tested (termed *A* through to *J* for each gene).

(B–E) qRT-PCR results for *Sox10*, *Olig2*, and *Nkx2-2* in MEF cells following co-transfection with gRNAs and dCas9-VP160 after 3 days (n = 3).

(B) *Sox10* targeted by single co-transfected gRNAs (*A*, *B*, *C*, etc.) compared with a pool of 10 gRNAs delivered simultaneously (n = 3; ordinary one-way ANOVA $p < 0.0001$). (C) *Olig2* targeted by single gRNAs (*A*, *B*, *C*, etc.) compared with a pool of 10 gRNAs delivered simultaneously (n = 3; ordinary one-way ANOVA $p < 0.0001$). (D) *Nkx6-2* targeted by single gRNAs (*A*, *B*, *C*, etc.) compared with a pool of 10 gRNAs delivered simultaneously (n = 3; ordinary one-way ANOVA $p < 0.0001$). (E) Transcription activation comparison of pools of ten or combinations of two or three gRNAs, co-transfected with dCas9-VP160, targeting *Sox10*, *Olig2*, or *Nkx6-2* (n = 3; unpaired t test). Negative control is transfection with dCas9-VP160 alone (No gRNAs).

(F) Immunofluorescent images for OLIG2 in non-transfected MEFs ("Control") and MEFs transfected with dCas9-VP160 and *G-I Olig2* gRNAs ("sTFs").

(G) Graphical representation of three all-in-one plasmids (SON, 2SON, and 3SON) containing dCas9-VP160 and increasing number of gRNAs targeting *Sox10*, *Olig2*, and *Nkx6-2* (top panel). qRT-PCR results for *Sox10*, *Olig2*, and *Nkx2-2* in MEF cells following delivery of all-in-one plasmids after 3 days (bottom panel) (n = 3; ordinary one-way ANOVA $p = 0.001$).

(H) Western blot demonstrating SOX10 and OLIG2 protein levels in MEFs 3 days after transfection with A1P-3SON plasmid ("3SON").

Statistical analysis—dots represent biological replicates, bars indicate means; error bar represent SD; unpaired t tests were performed. Statistical significance is marked by asterisks (*). See also Figure S2.

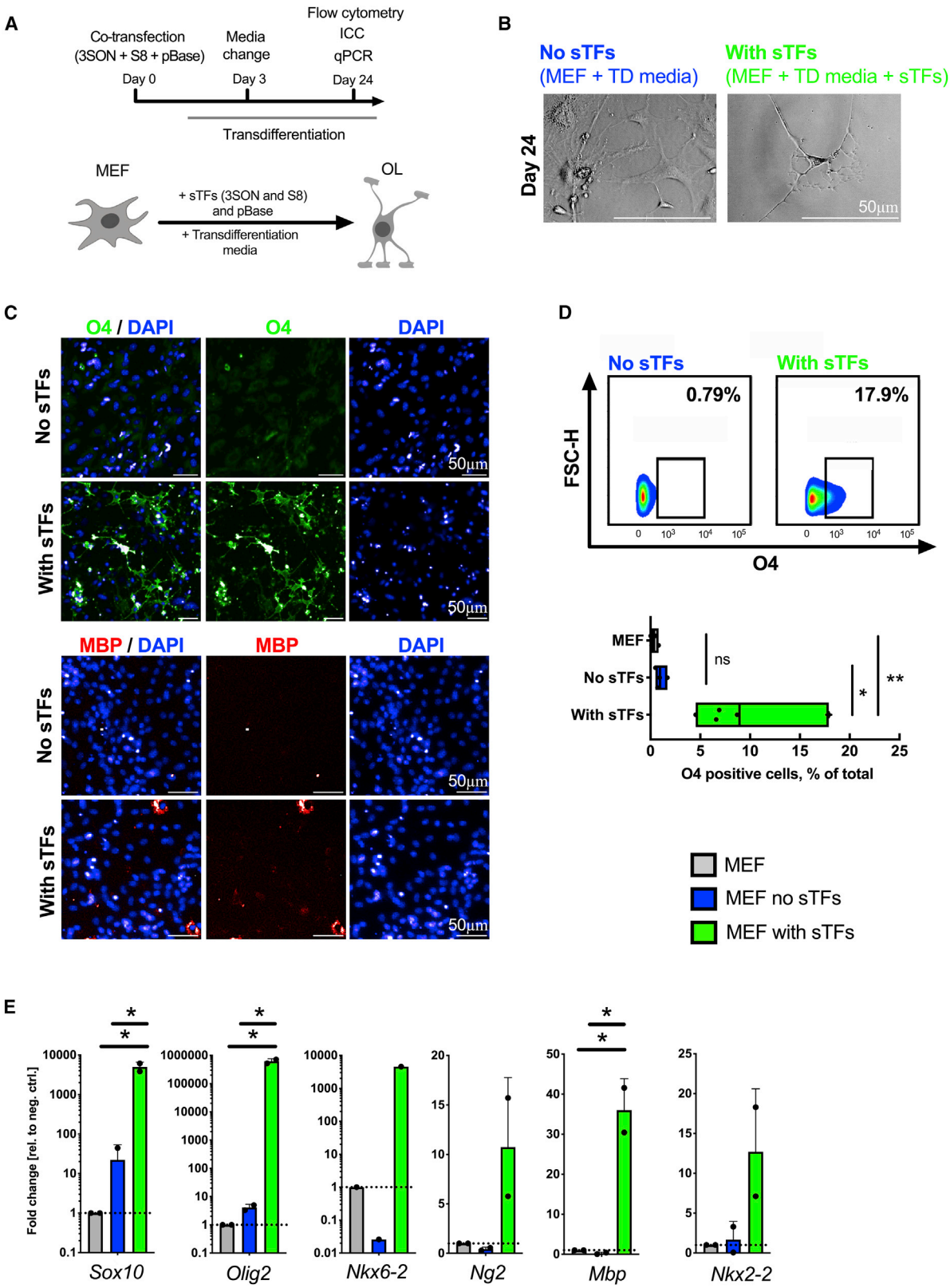

(legend on next page)

into either P2 (Figure 5C) or adult (Figure 5D) shiverer MBPshi/shi mice brain slices, cultured slices for another 10 days, and then stained for GFP and MBP (Figures 5C and 5D). In P2 brain slices, we observed engrafted GFP^+ cells with elaborate OL-like morphology, but they did not express MBP. In adult shiverer MBPshi/shi mice brain slices we observed partial colocalization of MBP and GFP staining (Figure 5D), suggesting that transdifferentiated cells can engraft and differentiate to generate MBP^+ sheaths, albeit with lower frequency compared with NSC- or ESC-derived OPCs (Figures 2I and S5D).

Next, we transplanted 5×10^5 transfected and TD medium-induced cells (via a bilateral injection of 2.5×10^5 cells), or non-transfected but TD medium-induced MEFs (negative control) into developing corpus callosum of P2 *Shiverer* (MBPshi/shi) mice (Figure 5E). We also tested OPCs derived from ESC differentiations as a positive control (Figure S5D). Twenty-one days later, mice were perfused, tissue was collected, and immunohistochemistry for MBP and neurofilament (NF) was performed on coronal brain sections to identify neurons (NF^+) and MBP^+ cells. Indeed, we identified a number of MBP-expressing cells near and around injection tracks in the mice that were transplanted with induced OL (iOL) (Figure 5F), but not in mice transplanted with control MEF cells (Figure S5E). However, we did not observe myelin sheath formations in iOL-transplanted mice, while ESC-derived OPCs were able to form myelin sheaths (Figure S5D). These data suggest that, while iOLs are able to engraft, and express O4 and MBP, they have some deficits that restrict their functional maturation with regards to myelination.

DISCUSSION

CRISPR/dCas9-based lineage programming and reprogramming has been reported previously for various lineages, but to our knowledge has not yet been explored in NSCs or fibroblasts for production of OLs. In this study we have shown the power of these tools when delivered as a single plasmid, to activate in multiplex several key master regulators of OL lineage. These were used to enhance NSC differentiation and MEF TD toward OLs. This study adds to a growing body of evidence showing that CRISPR/dCas9 can be used in cell fate programming, potentially improving on some more conventional methods such as cDNA overexpression.

When performing initial gRNA functionality screens in NSCs and MEFs, we found that only some of the sgRNAs were functional individually. Pooling multiple gRNAs (from 2 to 10) resulted in synergistic transcriptional activation. This is consistent with previous studies using sTFs—both TAL effector and dCas9 based (Black et al., 2016; Perez-Pinera et al., 2013). The most effective gRNAs we identified were within 130 bp and 300 bp from the TSS. One possible explanation for the synergy is that sTF binding/dissociation dynamics and, more importantly, transcription co-factor recruitment probability is increased due to increased number of sTFs around the accessible parts of the promoter. Although *Sox10* was amenable to activation in both MEFs and NSCs, *Nkx6-2* activation has worked only in MEFs. Interestingly, we find that even stronger effector domains, such as p300 or VPR, are not capable of overcoming the unknown biological barriers. Thus, for reprogramming studies our data suggest that multiple sgRNA need to be screened in the relevant host cell and potentially used as a pool to drive reliable and high levels of target gene expression.

We first tested sTFs in NSC differentiation context and demonstrated that *Sox10* activation alone can enhance NSC differentiation toward OPCs. A total of 15%–20% of differentiating NSCs (control) become OPCs. After we engineered these cells to express sTFs targeting *Sox10* for transcriptional activation, we recorded over 73% of OPCs after 4 days of differentiation. In comparison, overexpression of *SOX10* gave on average 52% of OPCs. A similar trend of

Figure 4. MEF Transdifferentiation to Induced Oligodendrocytes after sTF-Mediated Activation of *Sox10*, *Olig2*, and *Nkx6-2*

(A) Schematic summarizing the experimental strategy. MEFs were co-transfected with three plasmids, S8 (from Figure 2), 3SON (from Figure 3), and CAG-driven PiggyBac transposase. Three days later, transfected ("With sTF") and non-transfected MEFs ("No sTF") were incubated in transdifferentiation (TD) medium (see Experimental Procedures for details).

(B) Phase contrast images of non-transfected ("No sTFs") and transfected MEFs ("With sTFs") 24 days after transfection.

(C) Immunofluorescence images for O4 and MBP in non-transfected (No sTFs) and transfected (With sTFs) MEFs that have been cultured in TD medium, day 24.

(D) Typical example of flow cytometry data for $O4^+$ cells in MEFs that have been cultured in TD medium (No sTFs) and MEFs that have been transfected and cultured in TD medium (With sTFs), day 24. Quantification of flow cytometry data from 5 separate reprogramming experiments ($n = 5$; ordinary one-way ANOVA $p < 0.001$).

(E) qRT-PCR results for various lineage-specific markers in either MEFs (black), MEFs treated with OPC-permissive media (blue), and MEFs transfected with sTFs and treated with TD medium and sorted for O4 surface marker (green) at the end of a 24-day-long protocol ($n = 2$; unpaired t test).

Statistical analysis—dots represent biological replicates, bars indicate means; error bar represent SD; unpaired t-tests were performed. Statistical significance is marked by asterisks (*). See also Figure S5.

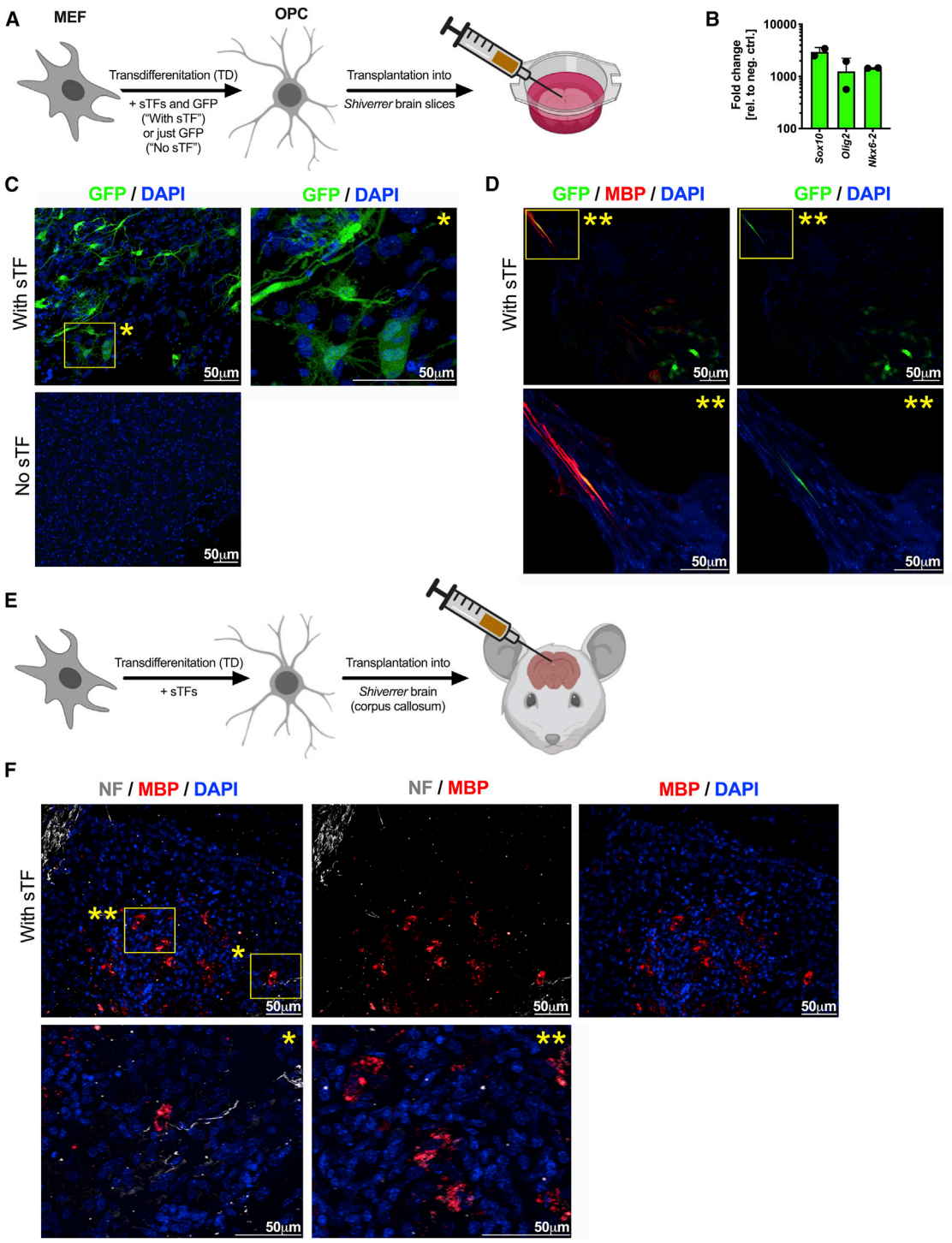

Figure 5. Transplantation of Reprogrammed iOLs to P2 or Adult *Shiverer* (MBPshi/shi) Mice or Mice Brain Slices

(A) Schematic summarizing the experimental strategy. Transfected and transdifferentiated MEFs were transplanted into *Shiverer* mice brain slices. Ten days after transplantations brain tissue section were stained.

(B) qRT-PCR results for *Sox10*, *Olig2*, and *Nkx6-2* in sTF-transfected cells before the transplantation (n = 2; unpaired t test).

(C) Immunohistochemistry for GFP in P2 *Shiverer* (MBPshi/shi) mice brain slices that were transplanted with cells transfected with sTF and GFP (With sTF) or just GFP (No sTF).

(legend continued on next page)

improved yields of $O4^+$ OLs was noted in a different NSC line. Although a significant enhancement of differentiating NSCs was achieved it was not a uniform response, suggesting further barriers to steering differentiation paths. It will now be interesting to investigate if activating a larger number of OPC/OL-specific genes, and/or repressing some NSC fate modulators (e.g., SOX2), would result in even more efficient or more rapid differentiation process.

To test if MEF TD could be initiated by sTFs, we needed activation of multiple genes with multiple sgRNAs and therefore we developed an improved plasmid-based strategy. This modular system is based on Golden Gate assembly, and allowed contruction of A1P, containing: PiggyBac ITR sequences, dCas9-VP160 (or other types of effector) and up to eight U6-sgRNA subunits. This provides a simple, yet flexible, system. Use of the piggyBac provides a means to generate stable genomic integration of the cassette with a possibility of excision if required (Wang et al., 2008). Although transfection-based delivery of piggyBac-based plasmids is less efficient compared with transduction-based lentivirus, lentivirus-based delivery is limited by restrictions to cargo size (maximum ±11 kb) and requires time-consuming and expensive viral production. To compensate for lower transfection/integration efficiencies of PiggyBac system it is possible to select positive cells via reporter gene inclusion. Although positive selection (using FACS or antibiotics) might be difficult for primary cells with lower replicative capacity, for those reprogramming experiments using proliferative starting cells (e.g., fibroblasts) the PiggyBac approach will be useful.

As ESC/iPSC differentiation relies on recapitulating the events that happened in an early embryo development, *in vitro* protocol that mimic these processes are inherently slow. The ultimate goal of CRISPR/dCas9 in cell fate reprogramming is to efficiently drive cell reprogramming in a reliable and rapid manner. One alternative to a cumbersome iPSC dedifferentiation-differentiation regime is direct cell fate programming (or TD) from one somatic cell to another. We demonstrated that TD can be initiated by activating multiple genes using two non-viral plasmids each containing dCas9-VP160 and eight U6-sgRNA subunits. The activation of three master regulator genes—*Sox10*, *Olig2*, and *Nkx6-2*—in MEFs using A1Ps provided ~9% conversion to OL-like cells. These cells were positive for O4, key markers of OPC lineage. Furthermore, we observed that once transplanted these reprogrammed OPCs were able to integrate into P2 or adult *Shiverer* (MBPshi/shi) mouse brain *in vivo* and *in vitro*, and express MBP—a known marker for mature myelinating OLs. However, in all myelination assays we could only observe a few MBP^+ cells and/or sheaths. This suggests that final maturation stage is incomplete in these reprogrammed cells. We believe that there could be a technical and/or biological explanation. Technically, maturation might be enhanced if cells were enriched for $O4^+$/OPC cells after TD and before transplantations. MBP^- cells seem to tightly surround reprogrammed MBP^+ cells, possibly preventing their interaction with NF^+ neurons (Figure 5F). Biologically, it might be also important to lower expression of some or all of the initial transcription factors (*Sox10*, *Olig2*, and *Nkx6-2*) to allow cells to reach maturation effectively. Currently, levels of transcripts remained high in transdifferentiated cells just before transplanting them (Figure 5B). Future studies and genome-wide transcriptional and epigenetic profiling in single cells will help define the roadblocks.

In future studies it will be interesting to push further the scale of multiplexing—perhaps activating transcription of tens or hundreds of genes at the same time—as this might be a key advantage of sTFs over more traditional ectopic overexpression methods in redirecting cell identity. Human artificial chromosomes could be used to deliver hundreds of sgRNAs and different versions of dCas9 into a single cell, allowing unprecedented multiplexing capacity (Martella et al., 2016). As the toolkit of CRISPR/Cas effectors expands it is likely that current sTF multiplexing capabilities will be expanded further by combining activators and repressors with chromatin editors. It will also be interesting to explore richer microenvironmental cues, such as scaffolds, or mechanical forces, which could help stimulate improved reprogramming and differentiation.

In conclusion, we have demonstrated sTF-mediated NSC directed differentiation as well as initiation of direct reprogramming of MEFs into OL-like cells. We have achieved such reprogramming events using a viral-free delivery strategy that enables activation of three separate genes in multiplex using up to eight sgRNA units. These sTFs clearly provide remarkable new tools that enable fundamental studies of reprogramming mechanisms and the transcriptional and

(D) Immunohistochemistry for GFP and MBP in adult *Shiverer* (MBPshi/shi) mice brain slices that were transplanted with cells transfected with sTF and GFP (With sTF).

(E) Schematic summarizing the experimental strategy. Transfected and transdifferentiated MEFs were transplanted into *Shiverer* mice at P2. Twenty-one days after transplantations, mice were perfused, coronal brain tissue sections were collected and staining was performed.

(F) Immunohistochemistry for MBP and NF in *Shiverer* (MBPshi/shi) P2 mice coronal brain slices of mice transplanted with cells transfected with sTF and GFP.

Statistical analysis—dots represent biological replicates, bars indicate means; error bar represent SD; unpaired t tests were performed. Statistical significance is marked by asterisks (*). See also Figure S5.

epigenetic barriers to lineage conversion. As we garner improved knowledge of the core transcriptional circuits and epigenetic programs that define each cell type and cell state, the *in vivo* resetting of mammalian cell-type identity using sTFs will likely drive considerable advances in regenerative medicine.

EXPERIMENTAL PROCEDURES

NSC Differentiation

NSCs were triggered to differentiate to OPCs using following differentiation protocols (Pollard, 2013). A day before differentiation, the cells were seeded at 2×10^4 cells per well of a 6-well plate. The next day, fresh culture medium lacking EGF but containing 10 μM Forskolin (Cambridge BioScience, no. 11018), 10 ng/mL PDGF-AA (R&D System, no. 221-AA-010) and FGF-2 (10 ng/mL) was added. Cells were left in such differentiation medium for 4 days, and then analyzed or induced to differentiate to OLs using the medium described below.

To differentiate OPCs to OLs, NSC culture medium lacking EGF and FGF, but containing 5% fetal calf serum (FCS) was used.

MEF TD Growth Medium and Protocol

MEFs were transdifferentiated to OPCs using the following protocol: cells were transfected (see below) and left in MEF culture medium for 3 days. After 3 days, the MEF culture medium was exchanged with MEF TD medium. TD medium contained the following DMEM/F12 (Invitrogen, no. 11320) supplemented with 1:100 N-2 (Life Technologies, no. 17502-048), 1:50 B-27 (Life Technologies, no. 17504-044), 2 mM GlutaMAX (Life Technologies, no. A1286001), 200 ng/mL SHH (R&D Systems, no. 461-SH-025/CF), 20 ng/mL FGF2 (R&D Systems), 20 ng/mL PDGF-AA (R&D Systems, no. 221-AA-010), and 2 μg/mL Laminin (Sigma).

To drive transdifferentiating MEFs to differentiate to MBP^+ OL, 21 days after transfection TD cells were incubated in the following medium for 3 days: DMEM/F12 (Invitrogen, no. 11320) supplemented 1:100 N-2 (Life Technologies, no. 17502-048), 1:50 B-27 (Life Technologies, no. 17504-044), 2 mM GlutaMAX (Life Technologies, no. A1286001), 40 ng/mL T3 (Sigma), 200 ng/mL SHH (R&D Systems, no. 461-SH-025/CF), 100 ng/mL Noggin (R&D Systems, no. 3344-NG-050), 50 μM cAMP (Sigma, no. D0260-5MG), 100 ng/mL IGF (R&D Systems, no. 291-G1-200), 10 ng/mL NT3 (R&D Systems, no. 267-N3-005/CF). This is based on the protocol previously published by Najm et al. (2013).

Immunofluorescence

Cells were washed with PBS and fixed with 4% paraformaldehyde (PFA) for 10 min at room temperature. After fixation, cells were washed three times with PBS. Cells were then blocked at least for 1 h in blocking solution (1% BSA, 3% goat serum, 0.1% Triton in PBS, unless stated otherwise). The blocking solution was removed and the primary antibody (anti-OLIG2 1:400, EMD Millipore, catalog no. 2367; anti-O4 1:200, Immunosolv [product discontinued]; anti-MBP 1:250, Bio-Rad, catalog no. MCA409S; anti-SOX2 1:100, Sigma, catalog no. S9072; anti-SOX9 1:100, EMD Milipore, catalog no. AB5535; anti-GFAP 1:1,000, Sigma, catalog no. G9269; anti-NESTIN 1:10, DSHB Hybridoma, catalog no. rat-401; anti-TUJ1 1:500, BioLegend, catalog no. 801202; anti-A2B5 1:100, Abcam, catalog no. ab53521) was added and incubated at 4°C overnight in blocking solution. After staining with primary antibody, cells were washed three times with PBST for 15 min. Cells were then stained with an appropriate secondary antibody (Alexa Fluor range; 1:1,000 dilutions) for at least 1 h in the dark at room temperature. Cells were washed two times with PBS, stained with DAPI (1:5,000 in PBS) for at least 5 min and washed with PBS twice.

Flow Cytometry

Cells were analyzed using an LSRFortessa 5- or 4-laser flow cytometer (BD Biosciences). Unless stated otherwise, 10,000 events were collected using forward scatter threshold of 5,000. Fluorescence data were collected using following cytometer settings: 488 nm laser and B530/30-A nm bandpass filter for GFP/NeoGreen, 561 nm laser and YG586/15-A nm bandpass filter for mRuby2/mCherry, 405 nm laser and V450/50-A nm bandpass filter for DAPI. DAPI staining was used to separate live and dead cells in every experiment. Data were analyzed using the FlowJo software.

When cell surface markers were assessed (O4), we immunostained live cells using the following protocol: cells were lifted with Accutase and incubated with PBS containing 1:200 Fc block CD16/CD32 (BD Pharmingen, no. 553141). Cells were left for 30 min at room temperature. After incubation, the cells were washed with 2% FCS/PBS and incubated with appropriately diluted (in 2% FCS/PBS) primary anti-O2 antibody (Immunosolv). Cells were left for 30 min at room temperature. After incubation, the cells were washed with 2% FCS/PBS and incubated with appropriately diluted (in 2% FCS/PBS) secondary antibody (Alexa Fluor range; 1:1,000). Cells were left for 30 min at room temperature in dark. After incubation, cells were washed with 2% FCS/PBS and analyzed with the flow cytometer.

In Vitro Myelination Assay with *Shiverer* Brain Slices

Slices were prepared essentially as described previously (Marqués-Torrejón et al., 2017). Postnatal day 2 or adult *Shiverer* mice were sacrificed and whole brains were embedded in agarose. Coronal brain slices (300 μm) were cut using a Vibratome (Leica). These were cultured for 3 days on a semi-permeable membrane cell culture insert (Millipore) using the following medium: 50% minimum essential medium α, 25% Hank's balanced salt solution, 25% horse serum, 6.5 mg/mL glucose, 2 mM glutamine, 1% N2 supplement, 1% P/S, 60 ng/mL T3, 25 μg/mL insulin, 20 μg/mL ascorbic acid, and 1 μM cAMP. After 3 days in cell culture, 2–4 μL of cell suspension (5×10^4 cells) was injected into brain slice. Slices were left for another 10 days to allow injected cell integration. Brain slices were then fixed with 4% PFA, washed with PBS, and stained with primary antibodies (anti-MBP 1:250, Bio-Rad, catalog no. MCA409S) for 2 days. Slices then were washed three times with PBS and stained with appropriate secondary antibody (Alexa Fluor range, 1:1,000) and DAPI for 4–6 h. Slices were washed with PBS and placed on glass slides. FluorSave (Milipore, no. 345789) was used to prevent photobleaching.

In Vivo Myelination Assay

All animal experiments were performed in line with UK Home Office guidelines. Under isoflurane anesthesia, P2 *Shiverer* MBPshi/shi mice received intracranial injection of 5×10^5 cells (via a bilateral injection of 2.5×10^5 cells) into the developing corpus callosum. MEFs, induced OPCs, or a positive control of mouse OPCs generated from ESCs were injected. Mice were perfused 21 days after injection. Tissue was collected and fixed in 4% PFA. Coronal sections (10 μm) were collected and blocked with 0.1% Triton X-100 (Sigma), 10% horse serum (Life Technologies) in PBS. Sections were incubated overnight at 4°C with rat anti-MBP (1:250, Bio-Rad, catalog no. MCA409S) followed by 1 h incubation with Alexa Fluor 568 goat anti-rat (1:1,000, Life Technologies, catalog no. A11077) and Hoechst (1:2,000, Thermo Fischer Scientific, catalog no. 62249). Slides were mounted and imaged on a Zeiss observer Z1. Images were processed using Zen software and ImageJ.

SUPPLEMENTAL INFORMATION

Supplemental Information can be found online at https://doi.org/10.1016/j.stemcr.2019.10.010.

AUTHOR CONTRIBUTIONS

M.M. led the majority of experimental studies. L.W. contributed to *in vivo* experiments. M.M., A.W. and S.M.P. were involved in design of the study. B.B. created the PDGFRA reporter line. C.B., S.B. and A.M. provided technical assistance. M.M. and S.M.P. wrote the manuscript. S.M.P. conceived the study.

ACKNOWLEDGMENTS

We thank Raul Bressan, Pooran Singh Dewari, and Sally Lowell for helpful comments on the manuscript. The authors thank Bertrand Vernay for help with microscopy, Fiona Jackson and Claire Cryer for help with flow cytometry, Amanda Boyd and A.W. for *Shiverer* mice, Matthew Swire and Charles ffrench-Constant for the O4 antibody. Colin Plumb provided help with MEF production. The project was supported by the BBSRC/EPSRC/MRC Synthetic Biological Research Center (BB/M018040/1), part of the UK Research Councils' investment in "Synthetic Biology for Growth." S.M.P. is a Cancer research UK Senior Research Fellow (A17368).

Received: January 14, 2019
Revised: October 12, 2019
Accepted: October 13, 2019
Published: November 7, 2019

REFERENCES

Balboa, D., Weltner, J., Eurola, S., Trokovic, R., Wartiovaara, K., and Otonkoski, T. (2015). Conditionally stabilized dCas9 activator for controlling gene expression in human cell reprogramming and differentiation. Stem Cell Reports *5*, 448–459.

Black, J.B., Adler, A.F., D'Ippolito, A.M., Leong, K.W., and Gersbach, C.A. (2016). Targeted epigenetic remodeling of endogenous loci by CRISPR/Cas9-based transcriptional activators directly converts fibroblasts to neuronal cells. Cell Stem Cell *19*, 406–414.

Chakraborty, S., Ji, H., Kabadi, A.M., Gersbach, C.A., Christoforou, N., and Leong, K.W. (2014). A CRISPR/Cas9-based system for reprogramming cell lineage specification. Stem Cell Reports *3*, 940–947.

Chavez, A., Scheiman, J., Vora, S., Pruitt, B.W., Tuttle, M., P R Iyer, E., Lin, S., Kiani, S., Guzman, C.D., Wiegand, D.J., et al. (2015). Highly efficient Cas9-mediated transcriptional programming. Nat. Methods *12*, 326–328.

Cheng, A.W., Wang, H., Yang, H., Shi, L., Katz, Y., Theunissen, T.W., Rangarajan, S., Shivalila, C.S., Dadon, D.B., and Jaenisch, R. (2013). Multiplexed activation of endogenous genes by CRISPR-on, an RNA-guided transcriptional activator system. Cell Res. *23*, 1163–1171.

Conti, L., Pollard, S.M., Gorba, T., Reitano, E., Toselli, M., Biella, G., Sun, Y., Sanzone, S., Ying, Q.L., Cattaneo, E., and Smith, A. (2005). Niche-independent symmetrical self-renewal of a mammalian tissue stem cell. PLoS Biol. *3*, e283.

Franklin, R.J.M., and Ffrench-Constant, C. (2017). Regenerating CNS myelin—from mechanisms to experimental medicines. Nat. Rev. Neurosci. *18*, 753–769.

García-León, J.A., Kumar, M., Boon, R., Chau, D., One, J., Wolfs, E., Eggermont, K., Berckmans, P., Gunhanlar, N., de Vrij, F., et al. (2018). SOX10 single transcription factor-based fast and efficient generation of oligodendrocytes from human pluripotent stem cells. Stem Cell Reports *10*, 655–672.

Gilbert, L.A., Larson, M.H., Morsut, L., Liu, Z., Brar, G.A., Torres, S.E., Stern-Ginossar, N., Brandman, O., Whitehead, E.H., Doudna, J.A., et al. (2013). CRISPR-mediated modular RNA-guided regulation of transcription in eukaryotes. Cell *154*, 442–451.

Gilbert, L.A., Horlbeck, M.A., Adamson, B., Villalta, J.E., Chen, Y., Whitehead, E.H., Guimaraes, C., Panning, B., Ploegh, H.L., Bassik, M.C., et al. (2014). Genome-scale CRISPR-mediated control of gene repression and activation. Cell *159*, 647–661.

Glaser, T., Pollard, S.M., Smith, A., and Brüstle, O. (2007). Tripotential differentiation of adherently expandable neural stem (NS) cells. PLoS One *2*, e298.

Goldman, S.A. (2016). Stem and progenitor cell-based therapy of the central nervous system: hopes, hype, and wishful thinking. Cell Stem Cell *18*, 174–188.

Hamilton, T.G., Klinghoffer, R.A., Corrin, P.D., and Soriano, P. (2003). Evolutionary divergence of platelet-derived growth factor alpha receptor signaling mechanisms. Mol. Cell. Biol. *23*, 4013–4025.

Hilton, I.B., D'Ippolito, A.M., Vockley, C.M., Thakore, P.I., Crawford, G.E., Reddy, T.E., and Gersbach, C.A. (2015). Epigenome editing by a CRISPR-Cas9-based acetyltransferase activates genes from promoters and enhancers. Nat. Biotechnol. *33*, 510–517.

Keung, A.J., Joung, J.K., Khalil, A.S., and Collins, J.J. (2015). Chromatin regulation at the frontier of synthetic biology. Nat. Rev. Genet. *16*, 159–171.

Liu, P., Chen, M., Liu, Y., Qi, L.S., and Ding, S. (2018). CRISPR-based chromatin remodeling of the endogenous Oct4 or Sox2 locus enables reprogramming to pluripotency. Cell Stem Cell *22*, 252–261.e4.

Marqués-Torrejón, M.Á., Gangoso, E., and Pollard, S.M. (2017). Modelling glioblastoma tumour-host cell interactions using adult brain organotypic slice co-culture. Dis. Model. Mech. *11*, dmm031435.

Martella, A., Pollard, S.M., Dai, J., and Cai, Y. (2016). Mammalian synthetic biology: time for big MACs. ACS Synth. Biol. *5*, 1040–1049.

Martella, A., Matjusaitis, M., Auxillos, J., Pollard, S.M., and Cai, Y. (2017). EMMA: an extensible mammalian modular assembly toolkit for the rapid design and production of diverse expression vectors. ACS Synth. Biol. https://doi.org/10.1021/acssynbio.7b00016.

Najm, F.J., Lager, A.M., Zaremba, A., Wyatt, K., Caprariello, A.V., Factor, D.C., Karl, R.T., Maeda, T., Miller, R.H., and Tesar, P.J. (2013). Transcription factor-mediated reprogramming of fibroblasts to expandable, myelinogenic oligodendrocyte progenitor cells. Nat. Biotechnol. *31*, 426–433.

Perez-Pinera, P., Kocak, D.D., Vockley, C.M., Adler, A.F., Kabadi, A.M., Polstein, L.R., Thakore, P.I., Glass, K.A., Ousterout, D.G., Leong, K.W., et al. (2013). RNA-guided gene activation by CRISPR-Cas9-based transcription factors. Nat. Methods *10*, 973–976.

Pollard, S.M. (2013). In vitro expansion of fetal neural progenitors as adherent cell lines. Methods Mol. Biol. *1059*, 13–24.

Pozniak, C.D., Langseth, A.J., Dijkgraaf, G.J.P., Choe, Y., Werb, Z., and Pleasure, S.J. (2010). Sox10 directs neural stem cells toward the oligodendrocyte lineage by decreasing Suppressor of Fused expression. PNAS *107*, 21795–21800.

Stolt, C.C., Schlierf, A., Lommes, P., Hillgärtner, S., Werner, T., Kosian, T., Sock, E., Kessaris, N., Richardson, W.D., and Lefebvre, V. (2006). SoxD proteins influence multiple stages of oligodendrocyte development and modulate SoxE protein function. Dev. Cell *11*, 697–709.

Wang, W., Lin, C., Lu, D., Ning, Z., Cox, T., Melvin, D., Wang, X., Bradley, A., and Liu, P. (2008). Chromosomal transposition of PiggyBac in mouse embryonic stem cells. PNAS *105*, 9290–9295.

Wang, S., Bates, J., Li, X., Schanz, S., Chandler-Militello, D., Levine, C., Maherali, N., Studer, L., Hochedlinger, K., Windrem, M., and Goldman, S.A. (2013). Human iPSC-derived oligodendrocyte progenitors can myelinate and rescue a mouse model of congenital hypomyelination. Cell Stem Cell *12*, 252–264.

Yang, N., Zuchero, J.B., Ahlenius, H., Marro, S., Ng, Y.H., Vierbuchen, T., Hawkins, J.S., Geissler, R., Barres, B.A., and Wernig, M. (2013). Generation of oligodendroglial cells by direct lineage conversion. Nat. Biotechnol. *31*, 434–439.

Zhang, S.C. (2001). Defining glial cells during CNS development. Nat. Rev. Neurosci. *2*, 840–843.